

using all available data between 1985 to 1994. Hence, sampling biases due to station density that changed over time can not be excluded.

The quarterly concentration pattern of PM_{10} is shown in Figure 6-18. The high sampler density allows the resolution of spatial texture on the scale of 100 km, particularly over major metropolitan areas. However, remote regions in the central and western states have poor spatial density. In the absence of rural monitoring data computerized contour plotting of PM_{10} is biased toward extrapolating (spreading) high concentrations over large areas. This bias is particularly evident in the maps for Quarters 1 and 4 in the western states, where the area of high concentration hot spots is exaggerated.

The AIRS PM_{10} concentrations over the eastern United States are lowest during Quarter 1, ranging between 20 to 30 $\mu g/m^3$. The higher concentrations exceeding 30 $\mu g/m^3$ are confined to metropolitan areas.

6.3.2.1 National Pattern and Trend of Aerometric Information Retrieval System PM_{10}

Two trend analysis approaches were used to obtain the 1988 to 1993 trends in PM_{10} shown in Figure 19b are subsequent figures providing AIRS concentration patterns. One of these approaches uses all of the available stations operational each year between 1988 and 1994. The second approach uses only those stations operational from 1988 to 1994, the long term coverage, trend, stations.

During the 1988 to 1994 period there were decreases in the annual average PM_{10} for the continental U.S. from 33 $\mu g/m^3$ to 25 $\mu g/m^3$, for all sites and from 35 $\mu g/m^3$ to 28 $\mu g/m^3$ for trend sites resulting in 24% or 20% reductions in PM_{10} .

The Figure 6-19b also shows the standard deviation among the yearly average PM_{10} concentrations for each year. On the national scale the standard deviation of yearly average concentrations is about 40% of the mean.

The concentrations of $PM_{2.5}$ and PM_{10} are compared in the scatter chart in Figure 6-19c. Each point represents a pair of $PM_{2.5}$ - PM_{10} monthly average concentrations. The diagonal line is the 1:1 line and shows the fine particle concentration ranges between 20 and 85% of PM_{10} . The heavy solid line is derived from a linear best fit regression. The detailed correlation statistics is reproduced in the upper-left corner of the scatter charts. The

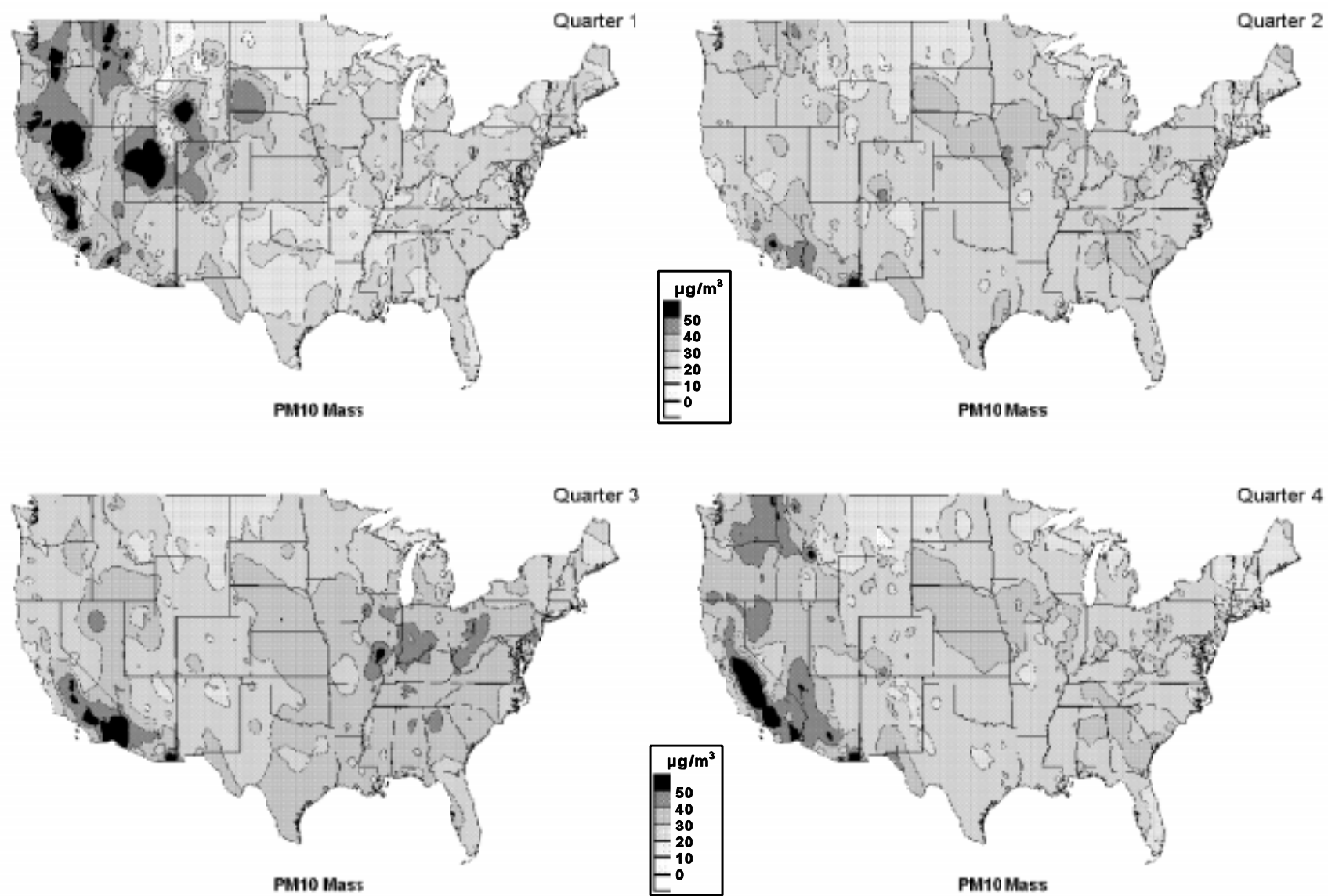


Figure 6-18. AIRS PM₁₀ quarterly concentration maps using all available data.

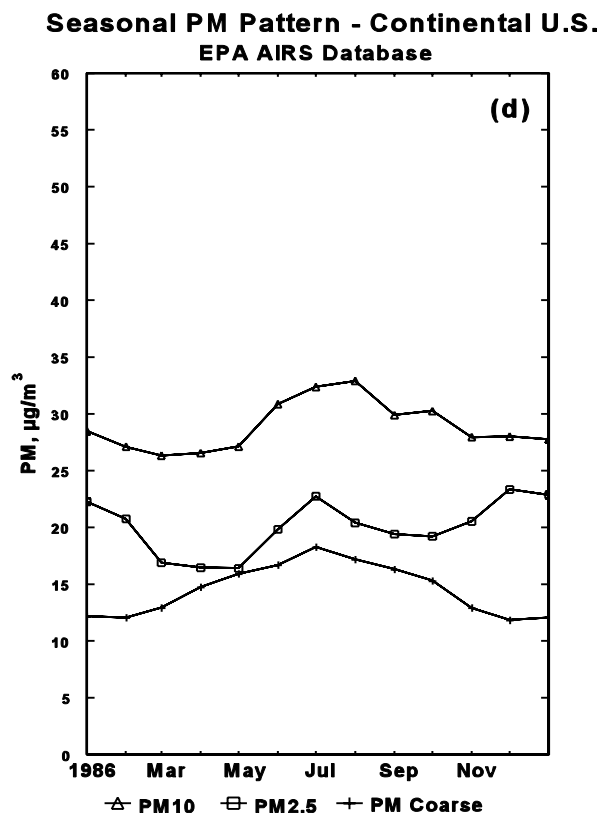
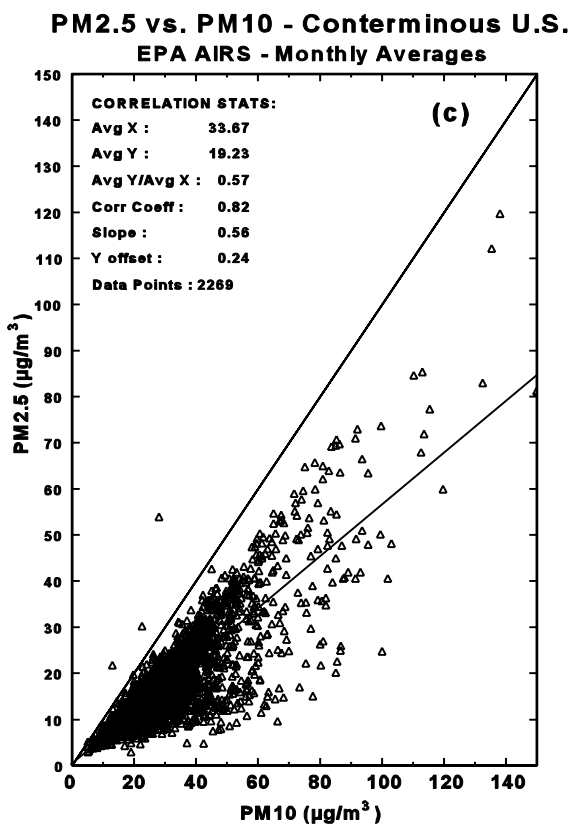
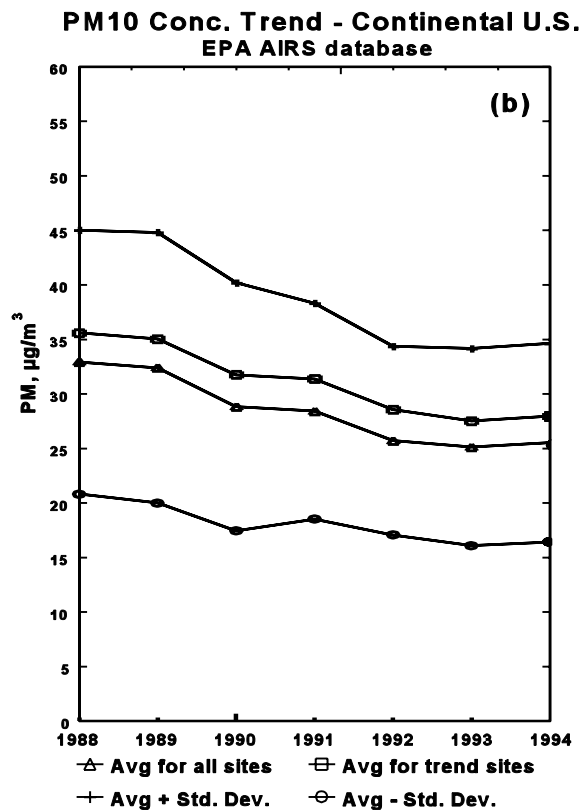


Figure 6-19. AIRS PM₁₀ and PM_{2.5} concentration patterns for the conterminous United States.

ratio of overall average $PM_{2.5}$ and overall average PM_{10} is also indicated. For the data when both $PM_{2.5}$ and PM_{10} data were available, nationally aggregated $PM_{2.5}$ particles accounted for 57% of the PM_{10} mass.

The seasonal pattern of the national PM_{10} concentration is also depicted in Figure 6-19d, utilizing all available data in AIRS. The national average PM_{10} seasonality ranges between $27 \mu g/m^3$ in March and April, and $33 \mu g/m^3$ in July and August, yielding a modest 16% seasonal modulation. There is also evidence of slight bimodality with the December through January peak.

The seasonal chart also shows the annual variation of $PM_{2.5}$, and $PM_{10}-PM_{2.5}$ (i.e., coarse particles). The national fine particle concentration shows clear evidence of bimodality with peaks in July and December. It is shown below that the fine particle winter peak arises from western sites, while the summer peak is due to eastern U.S. contributions. The national average coarse particle concentration has a 50 % yearly modulation with a single peak in July.

Stratifying the national PM_{10} concentrations one can obtain results showing that the country has several major aerosol regions, as discussed in more detail below. Each region has a discernible geographic extent as well as seasonal pattern. Over the plains of the eastern United States the spatial texture of PM_{10} is driven by the pattern of the emission fields, while the seasonality of concentrations is likely to be determined by the chemical transformation and removal processes, as well as by the regional dilution. In the mountainous western and Pacific states, pockets of wintertime PM_{10} concentrations exist that well exceed the eastern U.S. values. It is believed that haze and smoke in confined mountain valleys and air basins are strongly influenced by topography which in turn influences the emission pattern, dilution, as well as the chemical transformation and removal rate processes.

Given the regionality of the aerosol concentration pattern much of the discussion that follows will be focused on the characteristics of these aerosol regions. The Rocky Mountains produce a natural division between the eastern and western aerosol regimes which will be discussed next.

6.3.2.2 Eastern U.S. PM₁₀ Pattern and Trend

During the 1988 to 1994 period there were decreases in the annual average PM₁₀ for the eastern U.S. from 31 $\mu\text{g}/\text{m}^3$ to 26 $\mu\text{g}/\text{m}^3$ for all sites and from 34 $\mu\text{g}/\text{m}^3$ to 28 $\mu\text{g}/\text{m}^3$ for trend sites resulting in 16% or 18% reductions in PM₁₀ (Figure 6-20b). The decline is rather steady over time.

The highest eastern U.S. AIRS PM₁₀ concentrations are recorded in Quarter 3 (Figure 6-20d). The peak concentrations are over the Ohio River Valley stretching from Pittsburgh to West Virginia, southern Indiana and St. Louis. In this region, the PM₁₀ concentration over the industrialized Midwest during the summer can exceed 40 $\mu\text{g}/\text{m}^3$. Additional hot-spots with > 40 $\mu\text{g}/\text{m}^3$ are recorded in Birmingham, AL, Atlanta, GA, Nashville, TN, Philadelphia, PA and Chicago, IL. The summertime PM₁₀ concentrations in New England and upstate Michigan are < 20 $\mu\text{g}/\text{m}^3$.

The transition seasons Quarters 2 and 4 (Figure 6-20d) show PM₁₀ concentrations ranging from 25 $\mu\text{g}/\text{m}^3$ to about 30 $\mu\text{g}/\text{m}^3$ over much of the eastern U.S., with concentration hot-spots over the industrial Midwest as well as in the Southeast, Atlanta, GA and Birmingham, AL. The PM₁₀ concentrations in urban-industrial “hot-spots” exceed their rural surrounding by less than a factor of two.

The spatial variability of PM₁₀ occurring over the eastern United States is driven primarily by the varying primary aerosol emission density. This can be deduced from the coincidence of higher concentrations within urban industrial areas. The atmospheric dilution (i.e., horizontal and vertical dispersion) in these areas is not likely to be spatially variable. Also, the chemical aerosol formation and removal processes are likely to have weak spatial gradients when averaged over a calendrical quarter. Hence, the main factor that is believed to be responsible for the spatial variability is the emission field of primary PM₁₀ particles and the SO₂, NO_x, and VOC precursors of secondary aerosols.

PM₁₀ concentration in excess of 30 $\mu\text{g}/\text{m}^3$ is recorded over the agricultural states of Iowa, Kansas, Nebraska, and South Dakota. The elevated PM₁₀ concentrations over this region tend to persist over all four seasons. The eastern PM₁₀ seasonality (Figure 6-20d) is rather pronounced, with winter concentrations (December through March) of 24 $\mu\text{g}/\text{m}^3$, and

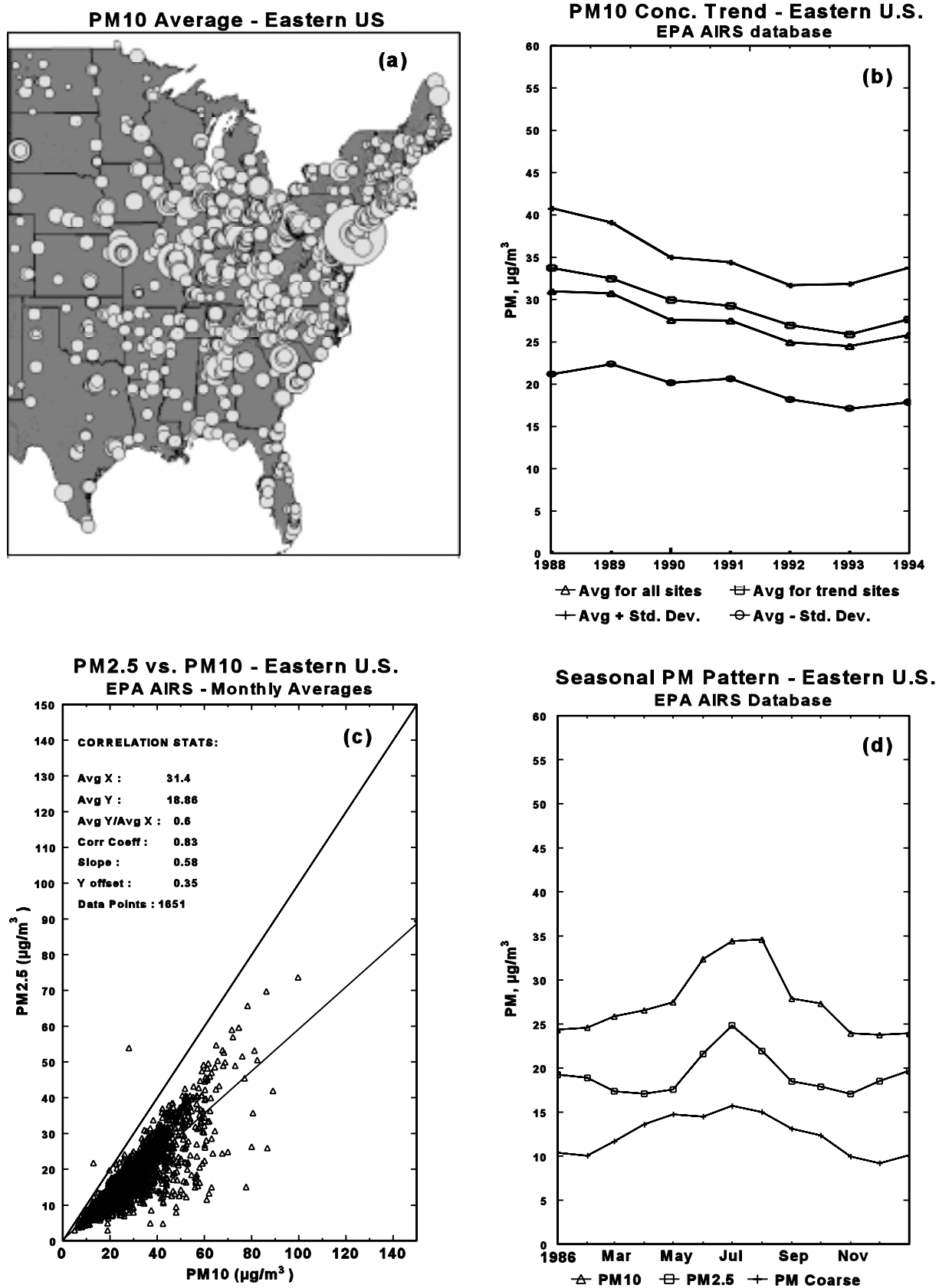


Figure 6-20. AIRS concentration data for east of the Rockies: (a) monitoring locations; (b) PM_{10} concentration trends; (c) PM_{10} and $PM_{2.5}$ relationship; and (d) PM_{10} , $PM_{2.5}$, and PM_{Coarse} seasonal pattern.

July through August peak of $35 \mu\text{g}/\text{m}^3$. The amplitude of the PM_{10} seasonal concentrations is about 30%.

The scatter chart of the eastern AIRS $\text{PM}_{2.5}$ - PM_{10} relationship shows a significant amount of scatter, with a slope of 0.58 (Figure 6-20b). The ratio of the overall average $\text{PM}_{2.5}$ and PM_{10} concentration is 0.6 such that 60% of PM_{10} is in the sub $2.5 \mu\text{m}$ size range. The seasonality of the fine AIRS particle concentration over the East is bimodal with a major peak in July and a smaller winter peak in January (Figure 6-20d). As shown in Figure 6-15b, the nonurban IMPROVE/NESCAUM network results for the eastern U.S. for $\text{PM}_{2.5}$ show a peak in summer but does not show a winter peak. The coarse particle concentration shows a single broad peak over the warm season, April through October (Figure 6-20d), but with a somewhat different pattern than shown in Figure 6-15b for nonurban cities in the eastern U.S. It is therefore evident that fine and coarse particles (from urban and nonurban measurements) have different seasonal dynamics in the East.

6.3.2.3 Western U.S. PM_{10} Pattern and Trend

The mountainous states, west of the Rockies (Figure 6-21) have higher PM_{10} concentrations in Quarters 1 and 4 than in Quarters 2 and 4 and shown even higher PM_{10} concentrations ($>50 \mu\text{g}/\text{m}^3$) at localized hot-spots. These higher concentrations occur over both metropolitan areas such as Salt Lake City, as well as in smaller towns in mountain valleys of states west of the Rockies.

The main geographic feature regions considered in California are the Los Angeles basin and the San Joaquin Valley. Both basins show monthly PM_{10} concentrations sometimes in excess of $50 \mu\text{g}/\text{m}^3$. These basins are also confined by surrounding mountains that limit the dilution, facilitate cloud formation, and have emissions that are confined to the basin floor. Accordingly, they represent airsheds with characteristic spatial and temporal pattern. It is likely that the actual local effects on the PM_{10} concentration field in the mountainous western states are greater than depicted in Figure 6-21a.

It appears that the spatial pattern of these high concentration hot spots is driven by emissions as well as by the restricted wintertime ventilation due to mountainous terrain. Over the mountainous western states the atmospheric dilution by horizontal and vertical dispersion is

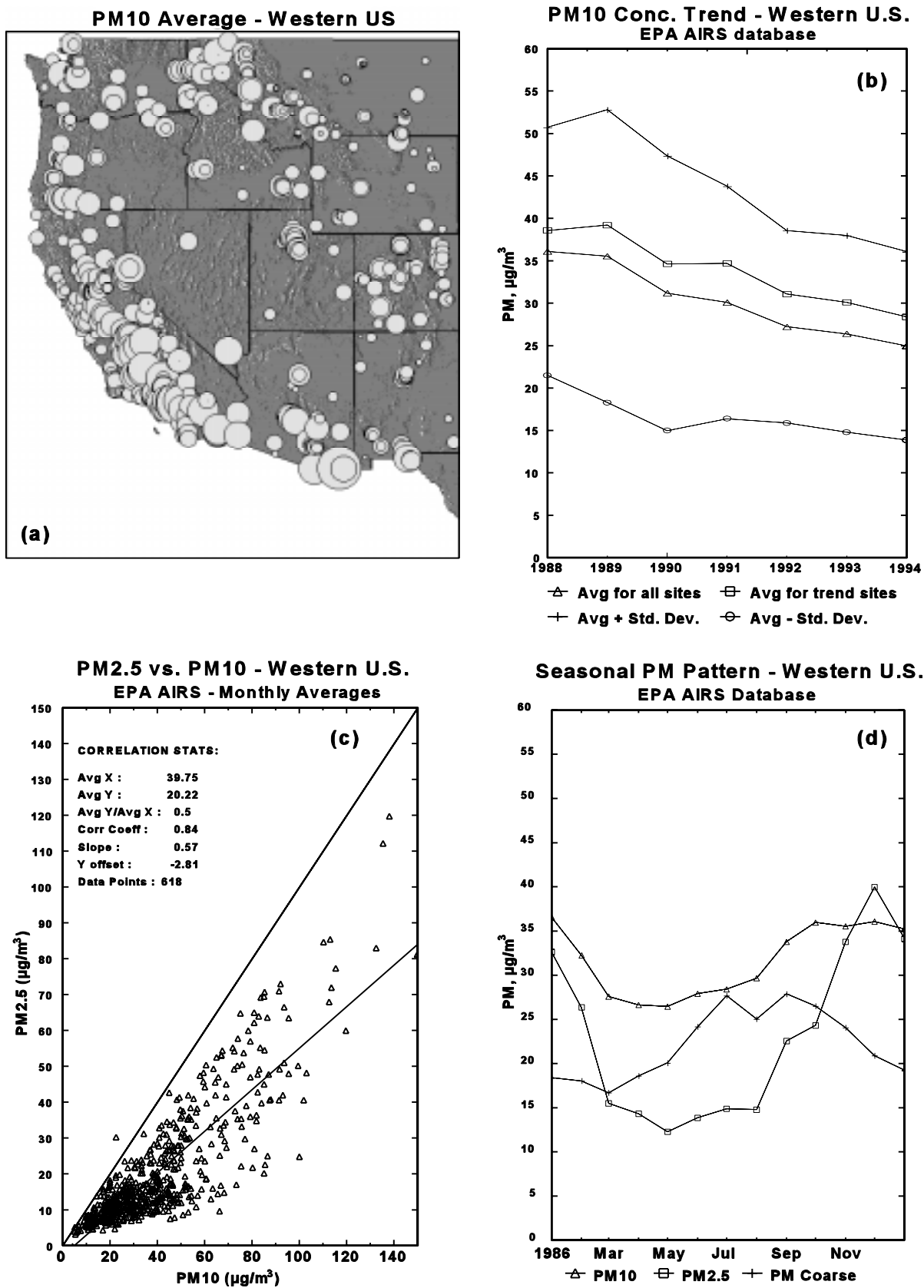


Figure 6-21. AIRS concentration data for west of the Rockies: (a) monitoring trends; (b) PM_{10} concentration trends; PM_{10} and $PM_{2.5}$ relationship; and (d) PM_{10} , $PM_{2.5}$, and PM_{Coarse} seasonal pattern.

severely restricted by mountain barriers and atmospheric stratification due to strong and shallow inversions. Radiative cooling also causes fog formation which enhances the production rate of hygroscopic aerosols in the valleys. As a consequence, mountain tops are generally protruding out of haze layers. Emissions arising from industrial, residential, agricultural, unpaved roadways and other sources are generally confined to mountain valleys. In the wintertime the mountain valleys are frequently filled with fog. All three major factors that determine the ambient concentrations (i.e., emissions, dilution, and chemical rate processes) are strongly influenced by the topography. For this reason, many of the maps depicting the regional pattern use shaded topography as a backdrop.

In the western half of the U.S., west of and including the Rockies, there was a decrease in the PM_{10} concentration of 1988 to 1994 from $36 \mu\text{g}/\text{m}^3$ to $25 \mu\text{g}/\text{m}^3$ for all sites and from $39 \mu\text{g}/\text{m}^3$ to $28 \mu\text{g}/\text{m}^3$ for trend sites (Figure 6-21b). The reductions were 31% for all sites and 28% for trend sites. Standard deviation among the western stations of yearly average PM_{10} concentrations is about 40%.

The western AIRS $PM_{2.5}$ - PM_{10} relationship (Figure 6-21c) shows that on the average about 50% of the PM_{10} is contributed by fine particles. The scatter of data points (Figure 6-21c) also shows that during high concentration PM_{10} episodes the fine fraction dominates.

The western PM_{10} seasonality (Figure 6-21d) is also rather pronounced, having about 30% amplitude. However, the lowest concentrations ($26 \mu\text{g}/\text{m}^3$) are reported in the late spring (April through June), while the highest values occur in late fall (October through January).

The seasonality of $PM_{2.5}$ west of the Rockies (Figure 6-21d) is strongly peaked in November through January. In fact, the $PM_{2.5}$ is several times higher than the summertime values. On the other hand, the coarse fraction shows a broad peak during late summer, July through October. It is to be noted that in Figures 6-20 and 6-21, the fine and coarse particle concentrations do not add up to PM_{10} , because size resolved samples were only available for tens of sites, while the PM_{10} concentrations were obtained from hundreds of monitoring stations.

In summary, there is a 20 to 24% reduction of PM_{10} concentrations for the continental U.S. between 1988 and 1993. On the national average the PM_{10} seasonality is weak. Desegregation of the national averages into east and west of the Rockies, shows that the downward trend west of the Rockies is more pronounced than over the eastern half of the U.S. The east-west desegregation also shows that the lack of national PM_{10} seasonality arises from two strong

seasonal signals that are phase shifted, the eastern United States has a summer peak, the West a fall and winter peak, and the sum of two signals is a weakly modulated seasonal pattern. Nationally, $PM_{2.5}$ mass accounts for about 57% of PM_{10} mass. The East and West show comparable average fine particle fractions (60% in the East and 50% in the West). Fine particles tend to dominate during the fall and winter season in the western U.S., except in the southwest.

It is evident that further examination discussed in the next sections will show that the East-West division itself is rather crude and that dividing the conterminous United States into additional subregions is beneficial in explaining the PM_{10} concentration pattern and trends.

6.3.2.4 Short-Term Variability of PM_{10} Concentrations

The previous aerosol concentration patterns were expressed as quarterly averages. However, for health and other effects, the variance of the concentration, in particular the occurrence of extreme high concentrations is of importance. The PM_{10} concentrations exhibit marked differences in the shape of their distribution functions around the mean values. For example in Figure 6-22, the day to day variations of PM_{10} concentrations in Knoxville, TN are about 40% of the mean value of $35 \mu\text{g}/\text{m}^3$. On the other hand, the concentration time series for Missoula, MT shows a coefficient of variation of 60% over the mean of $34 \mu\text{g}/\text{m}^3$. During the winter season the coefficient of variation is even higher. It is therefore evident, that for comparable mean concentrations the Missoula, MT site exhibits significantly higher short-term variations. Also note the large variations from a high concentration day to the lower concentrations on the day before and/or the day after (Figure 6-22).

The variability of concentration is examined spatially and seasonally by computing logarithmic standard deviation (ratio of 84/50 concentration percentiles) for each monitoring site. These deviations were then contoured for each season. The results are depicted in the seasonal maps of the logarithmic standard deviation (Figure 6-23). The highest logarithmic standard deviation is recorded over the northern and northwestern states during the cold